Synthesis and X-ray diffraction studies of new photocatalyst $Zn_{1-x}Pb_xBi_2O_4$

M. Eddya, B. Tbib, K. El-Hami*

Laboratory of Nanoscience and Modeling, Polydisciplinary Faculty of Khouribga, University Hassan 1st, Morocco.

Abstract

Photocatalysis is based on the principle of activating a semiconductor using the energy provided by light. The semiconductor is considered as a catalyst. Its principle is close to heterogeneous catalysis where the oxidation-reduction reaction takes place on the surface of the catalyst. We want from this study to see the substitution effect of Zn^{2+} by Pb^{2+} with different concentrations on the crystal structure of $Zn_{1-x}PbxBi_2O_4$ (x=0.1, 0.2, 0.3, 0.4, 0.5) and also on the volume of its cell. the results show that the cell parameters can increase or decreases with increasing concentrations of Pb^{2+} due to different physical phenomenous inside cell. Photocatalyst $Zn_{1-x}PbxBi_2O_4$ (x=0.1, 0.2, 0.3, 0.4, 0.5) were synthesized by solid state method. All samples are characterized by X-ray diffraction (XRD), and Fourier transforms infrared spectroscopy (FTIR). The FTIR spectroscopy shows generally that transmittance decreases with increasing concentration of Pb^{2+} in materials.

1. Introduction

Semiconductor photocatalysis has attracted increasing attention for solar energy harvest just like dye-sensitized solar cells [1] and photocatalytic water splitting [2], and have attracted increasing attention owing to their magnetic, resistive, optical [3], electrical, catalytic, environmental remediation just like photocatalytic decomposition of pollutants in water and removal of toxic gas in the air [4] and electrochemical properties [5]. Among these semiconductors. The oxides of titanium (Ti), bismuth (Bi), zinc (Zn) and tin (Sn) are the prefered materials for the photocatalytic processes [6]. However, most of them generally have a wide band gap and relatively high recombination rate of electron–hole pairs, leading to a poor efficiency of photocatalytic reaction. They have been widely investigated for various applications such as water treatment as adsorbents of organic pollutants or heavy metal ions Pb^{2+} [7]. A variety of approaches have been explored to enhance the photocatalytic activity of photocatalysts, including composite [8], morphological control [9], chemisorption of industrial gases [10] ion doping [11], surface sensitization [12], noble metal loading [13], fuel and Li-air cells as electrocatalysts of oxygen or H_2O_2 reduction [14] and hetero structure constructing [15].

Incorporating Pb^{2+} ions into a spinel structure of $ZnBi_2O_4$ is a successful pathway to increase their physical, chemical properties, also the size of the grains of a material acts on its physicochemical performances, which often increases with the decrease of the size of the grains, and it is the objective of this study which showed that this substitution has an important effect on the properties $Zn_{1-x}Pb_xBi_2O_4$ spinel structure (x =0.0, 0.1, 0.2, 0.3, 0.4 and 0.5). Substitute with different Zn^{2+} cation of $ZnBi_2O_4$ spinel oxide (10%, 20%, 30%, 40 and 50%) by the Pb^{2+} cation to see the effect onstructural parameters sizes and bonds in material structure.

However, the preparation processes of these approaches are complicated to some degree; therefore, looking for a simple compound of high efficient degradation ability for organic pollutants has been in the spotlight of photocatalytic researches. Spinel-like mixed metal oxides, usually with a chemical formula of $A^{2+}B_2^{3+}O_4$, in this structure, all the A^{2+} ions occupy the tetrahedral sites and all B^{3+} ions occupy the octahedral sites.In this study A^{2+} present Zn^{2+} or Pb^{2+} ions after substitution, and B^{3+} present Bi^{3+} ions.

2. Material and Methods

Elaboration of the spinels compound $Zn_{1-x}PbxBi_2O_4$

The material $Zn_{1-x}Pb_xBi_2O_4$ is synthesized from Zinc oxide (ZnO), lead oxide (PbO) and Bismuth trioxide (Bi_2O_3) are in the solid-state. Precursors are provided by Aldrich company. The preparation of the base

compound $Zn_{1-x}Pb_xBi_2O_4$ is done by solid state method. We shall endeavor to describe the results obtained from the set of multi-scale characterizations performed on the different photocatalyst materials based exclusively on p-type semiconductors. The oxides Bi_2O_3, PbO and ZnO are weighed in the required stoichiometric proportions, then intimately mixed by thorough grinding in porcelain mortar until perfectly homogeneous mixture is obtained. This is subjected to first heating at T = 200 °C for 6 hours. At the end of this first heating, the mixture obtained is again finely ground for 20 minutes before being brought to the temperature of T = 400 °C for the same duration. All samples are then subjected to heating to 800 °C with grinding .

The chemical reaction equations are :

- For the synthesis of $ZnBi_2O_4$: $ZnO + Bi_2O_3 \longrightarrow ZnBi_2O_4$
- For the synthesis of $Zn_{1-x}Pb_xBi_2O_4$: $(1-x)ZnO + xPbO + Bi_2O_3 \longrightarrow Zn_{1-x}Pb_xBi_2O_4$

The experimental process is summarized in (Figure 1), and masses of each precursor are shown in Table 1.
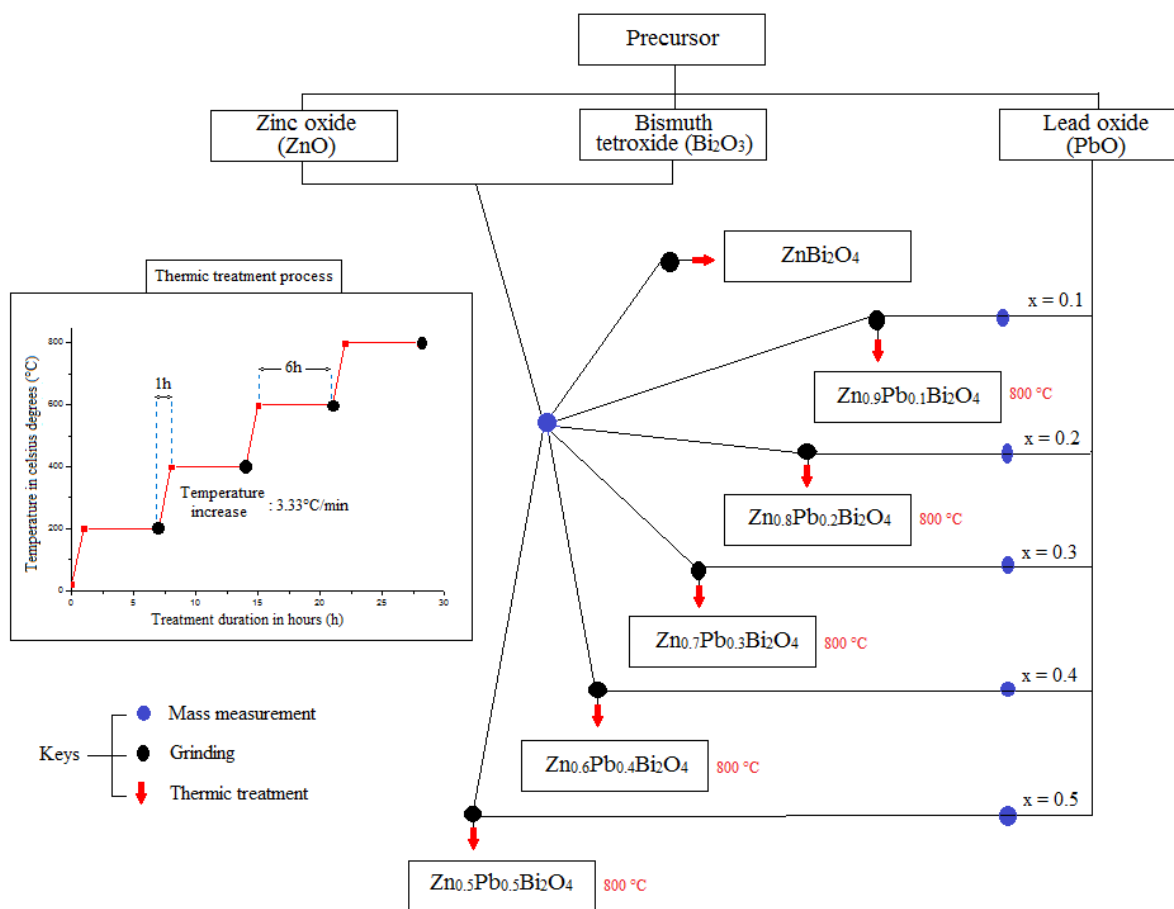
Figure 1 : Synthesis process for the elaboration of various $Zn_{1-x}Pb_xBi_2O_4$ (x=0.0, 0.1, 0.2, 0.3, 0.4 and 0.5) spinels by solid state method.

Table 1: Precursor mass for the elaboration of 1 g of various $Zn_{1-x}Pb_xBi_2O_4$ (x=0.0, 0.1, 0.2, 0.3, 0.4 and 0.5) spinels.

Precursors Chemical formula $Zn_{1-x}Pb_xBi_2O_4$	% of Substitution Zn^{2+} by Pb^{2+}	Zinc oxide (ZnO)	Lead oxide (PbO)	Bismuth tetroxide (Bi_2O_3)	Error of all weight ±
$ZnBi_2O_4$	x = 0.0 → 0 %	0.1487 g	0 g	0.8513 g	0.001 g
$Zn_{0.9}Pb_{0.1}Bi_2O_4$	x = 0.1 → 10 %	0.1304 g	0.0397 g	0.8298 g	0.001 g
$Zn_{0.8}Pb_{0.2}Bi_2O_4$	x = 0.2 → 20 %	0.1131 g	0.0775 g	0.8094 g	0.001 g
$Zn_{0.7}Pb_{0.3}Bi_2O_4$	x = 0.3 → 30 %	0.0966 g	0.1135 g	0.7899 g	0.001 g
$Zn_{0.6}Pb_{0.4}Bi_2O_4$	x = 0.4 → 40 %	0.0808 g	0.1478 g	0.7714 g	0.001 g
$Zn_{0.5}Pb_{0.5}Bi_2O_4$	x = 0.5 → 50 %	0.0658 g	0.1805 g	0.7537 g	0.001 g

3. Results and discussion

3.1. Structural characterizations

The structural analysis X-ray diffraction of $Zn_{1-x}Pb_xBi_2O_4$ powders was carried out by a Bruker type D8 AXS diffractometer apparatus, with copper anticathode ($\lambda CuK\alpha$ = 0.15406 nm). The recording condition is 0.02 °/20s for 2θ taken between 10° and 80°. The crystallographic parameters of all samples were refined from the experimental positions of the diffraction lines using the Fullprof program [16]. The X-ray spectrums indicate the good structural quality of our powders, due to one intense peaks with low numbers of secondary peaks. The reitveld refinement by fullprof software show that all our powders has an orthorhombic crystalin structure with Pmmm space group symmetry. Moreover, the spectrum does not include any additional line of sufficient intensity capable of belonging to any impurity, which indicates a good stability of all our powders. The table 2 summarize the crystallographic cell parameters and cell volumes results of our spinels structures with partial occupancy of both 1/8 of tetrahedral, and ½ of the octahedral sites. A spinel unit-cell is made up of eight FCC cells made by oxygen ions in the configuration 2×2×2, so it is a big structure consisting of 32 oxygen atoms, 8 Zn atoms and 16 Bi atoms. Depending on cations occupy different interstices. The spinel structure can be normal or inverse, see (Figure 2).
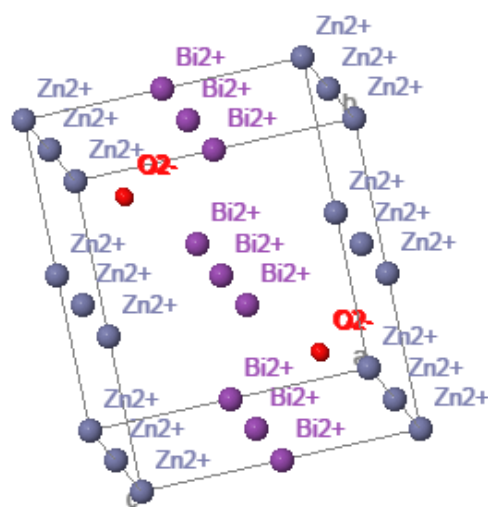
Figure 2 : Representation of the $ZnBi_2O_4$ compound.

For each spinels compound series, the evolution of cell parameters is monotonous of Pb^{2+} ion concentration (x) as shown in (Figure 3). We note that the variation of cell parameters of $Zn_{1-x}Pb_xBi_2O_4$ are according to percentage of lead substitution. We observe generally an increase of the cell parameters a,b and c. The parameter a increase in range x=0-x=0.5 with high increasement for x=0.1 and x=0.4. The b parameter has a continuous increasement following lead concentration from x=0 until x=0.5 except x=0.3. Also, the parameter c increase in range x=0.0-x=0.5 with a high increasement for x=0.2. We notice the short deacreasement of parameter b in x=0.3 lead concentration. These increasement of a,b,c parameters is due to Pb^{2+} radius, when we replaced Zn^{2+}(R(Zn^{2+})[coordinence-6]=0.74Å and R(Zn^{2+}[coordinence-4]= 0.6Å) by Pb^{2+} (R(Pb^{2+})[coordinence-6] = 1.18Å and R(Pb^{2+}[coordinence-4] = 0.94Å).

According to the radii, 0.44Å or 0.34Å of the length has been added respectively in our spinel cell when we replace each Zn^{2+} by Pb^{2+}. This reason, can explain the parameters increasement. However, we notice the decreasment of some parameters in some x range, this decreasement prove the non linear substitution of Zn^{2+} by Pb^{2+}, due to low lead concentration in cell wich exhibit a scattered distribution of Pb^{2+} in cell, wich cause some shrink of reticular planes. Also the attractive effect of the lead is more than that of the zinc, so the lead attract more electrons wich can cause reduce of cell parameters . The preferred orientation of reticular plan is other factor can cause a shrink or Stretch of cell [17] after lead incorporating into spinel structure wich give a possibility of increase or decrease of cell parameters. Also this increase or the decrease of the cell parameters, can be bound to the elasticity of the crystal lattice [18] trained by groupings bound only by summits. The reability factors result from rietveld refinement are reported in Table 3, and the experimental, calculated and differential spectra as shown in (Figure 4). This study show the strong effect of Zn^{2+} versus Pb^{2+} electronic configurations on the spinel structural parameters.
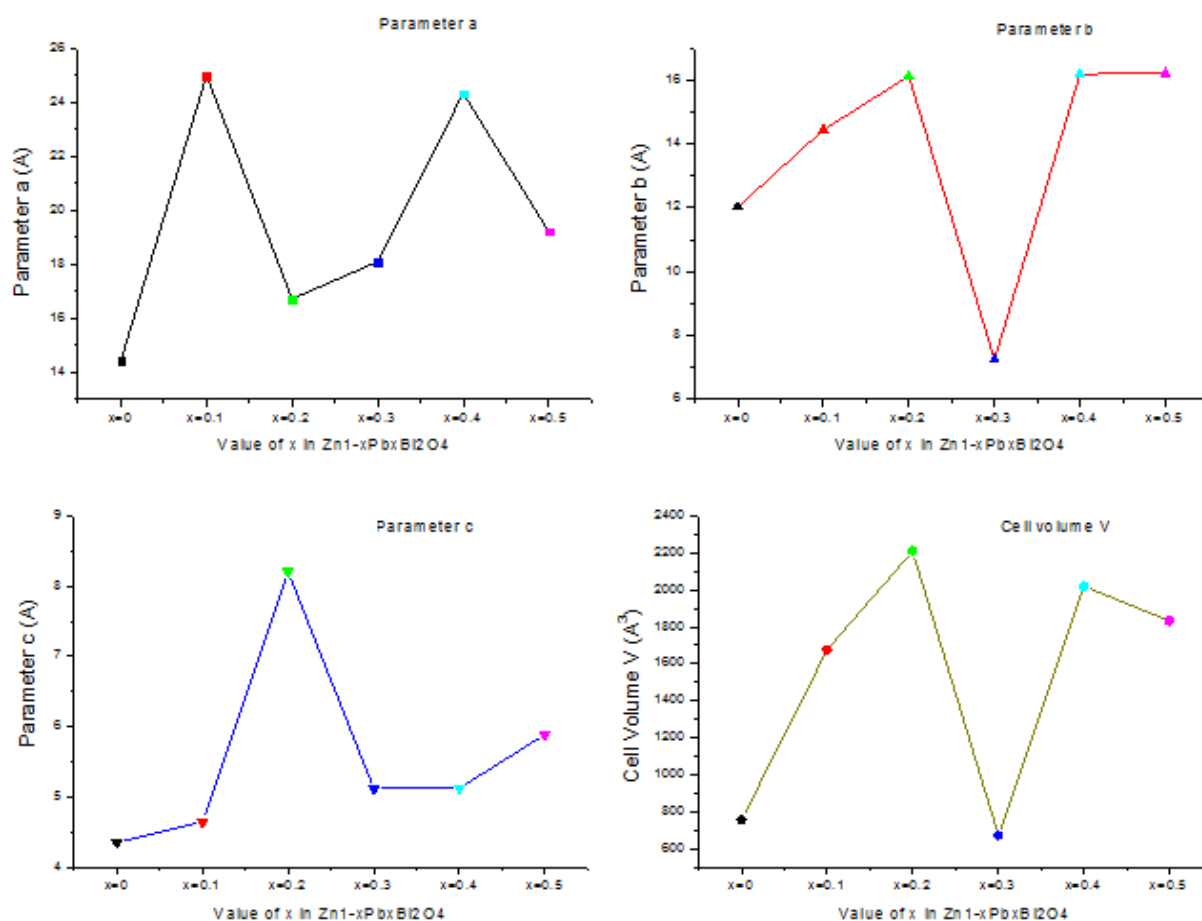
Figure 3 : Evolution of volume and cell parameters of all our spinel function x Pb^{2+} content .

Table 2 : Cell parameters extracted from full pattern refinements of various $Zn_{1-x}Pb_xBi_2O_4$ spinels

$Zn_{1-x}Pb_xBi_2O_4$	a (Å)	Error(Å) ±	b (Å)	Error(Å) ±	c (Å)	Error(Å) ±	$\alpha=\beta=\gamma(°)$	V (Å3)	Error(Å³) ±
x=0.0	14.4369	0.0010	12.0224	0.0010	4.3519	0.0010	90.00	755.3484	0.0010
x=0.1	24.9893	0.0010	14.4408	0.0010	4.6436	0.0010	90.00	1675.7090	0.0010
x=0.2	16.7116	0.0010	16.1244	0.0010	8.2069	0.0010	90.00	2211.4690	0.0010
x=0.3	18.0995	0.0010	7.24360	0.0010	5.1196	0.0010	90.00	671.1995	0.0010
x=0.4	24.3326	0.0010	16.1954	0.0010	5.1259	0.0010	90.00	2020.0050	0.0010
x=0.5	19.2020	0.0010	16.2124	0.0010	5.8874	0.0010	90.00	1832.8220	0.0010

Table 3 : Agreement factors of the Rietveld fitting for x =0 ,0.1, 0.2, 0.3, 0.4, 0.5

Pb content x	Rp (%)	Rwp (%)	Rexp(%)	Gof
0.0	12.6	18.9	9.17	2.06
0.1	12.6	18.2	12.32	1.47
0.2	11.0	13.8	5.77	2.4
0.3	10.1	15.2	9.51	1.60
0.4	10.3	15.4	8.86	1.74
0.5	14.0	28.2	10.21	2.76

This Rietveld analysis show clearly, following the reability factors: Rp (background subtracted) estimators, Rwp (revealing the profile) and Gof (overall quality factor) a good structural refinement with Rp,Rwp less than 15% and Gof near or less than 2. We note that three Rwp factors for x=0.0, x=0.1 and x=0.5 are more than 15%,

despite model change and profile refinement, reason to their spectrum, they need more XRD time analysis for having more spectrum quality. But their Gof factors is less than 2 for x=0.1 and near 2 for x=0.0 and x=0.5. Also the low difference between calculated and observed spectrum curve indicate the good refinement of all our spinels structure.
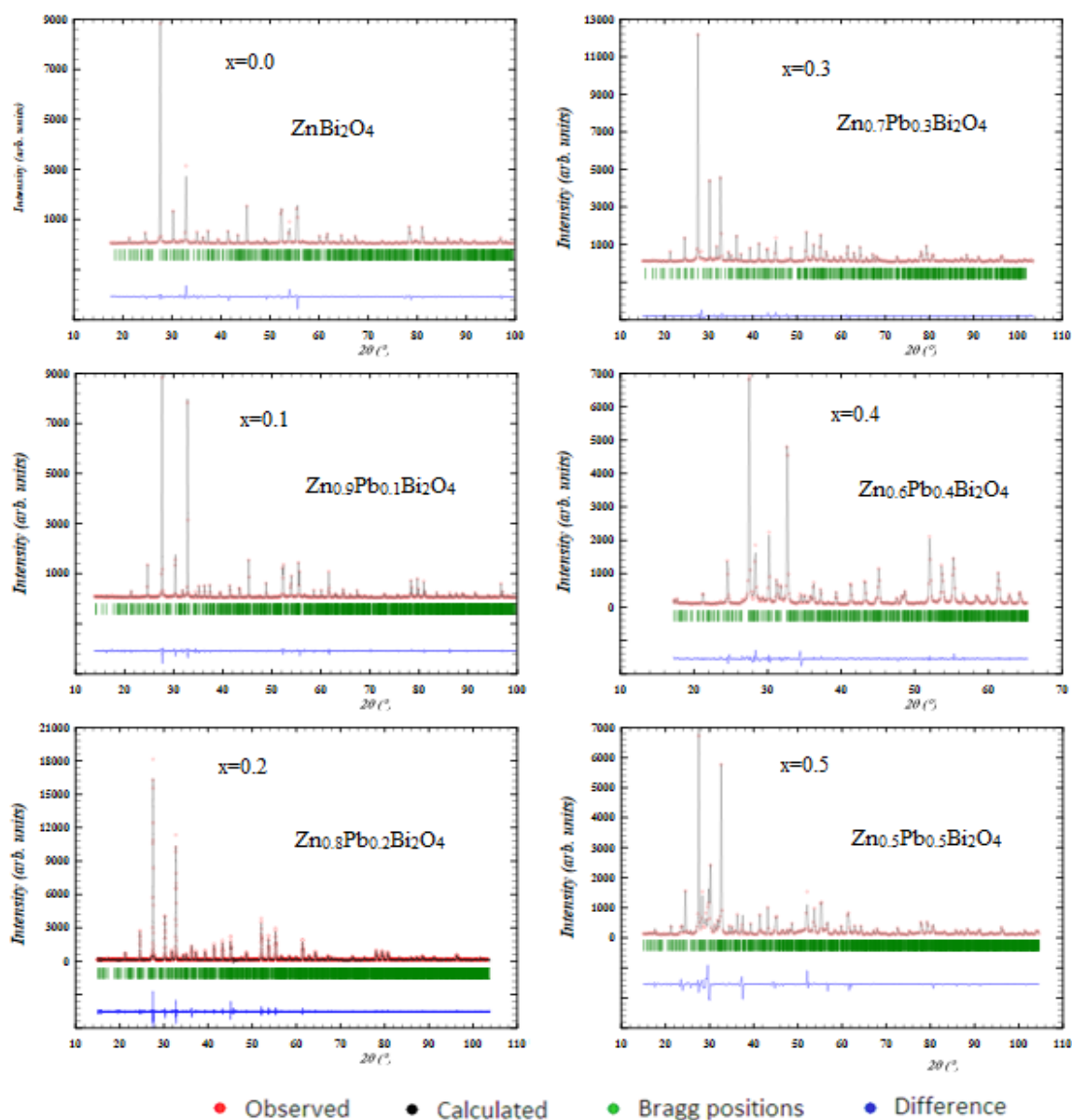
Figure 4: X-ray diffraction patterns of compounds $Zn_{1-x}Pb_xBi_2O_4$, x = 0.0, 0.1, 0.2, 0.3, 0.4, 0.5

3.2. Fourier transforms infrared spectroscopy (FTIR)

FTIR spectroscopy is an Optical technique that detects molecular bond vibrations and rotations upon absorption of infrared light [19]. Because different chemical functional groups absorb the infrared light at different frequencies [20] , FTIR spectroscopy can be used for chemical structure analysis, chemical fingerprinting and chemical imaging [21]. This absorption show the existence of bonds of some samples. The infrared spectrum represents the transmittance (T) on the ordinate, it is expressed as a percentage (%) according to the waves number, and is expressed in (cm^{-1}). We can see that the absorption strips are pointing downwards to a low transmission value corresponding to a high absorption and each band is characterized by its position, width and intensity.

FTIR spectroscopy thus provides both qualitative and quantitative information and is shown to be an effective companion technique to X-ray diffraction, The FTIR spectrum show also the bands arising from inter atomic vibrations. The structural changes brought by metal ions is strongly influenced the lattice vibrations. The lattice

vibrations also depend on the cations mass, the cation oxygen and the bonding force. The (Figure 5) show that our spinels oxide powders $Zn_{1-x}Pb_xBi_2O_4$ (x = 0, 0.1, 0.2, 0.3, 0.4, 0.5) manifests absorption peaks in the range of 400–4000 cm^{-1}. The inset indicates two absorption bands which is a common feature of all spinels. Two main absorption bands corresponding to the stretching vibration of the tetrahedral and octahedral sites are around 550 and 620 cm^{-1}, respectively. The tetrahedral bands are shifted from lower bands to higher bands 620 cm^{-1}, that can be ascribed to the shifting of Bi^{3+} ions towards oxygen ion on the tetrahedral site which decreases ($B^{3+}- O^{2-}$) distances. The band at 1375 cm^{-1} is attributed to the formation of Pb^{2+} substituted spinel bismuth Bi^{3+}. The band at 1625 cm^{-1} is ascribed to the presence of absorbed water (H–O–H).
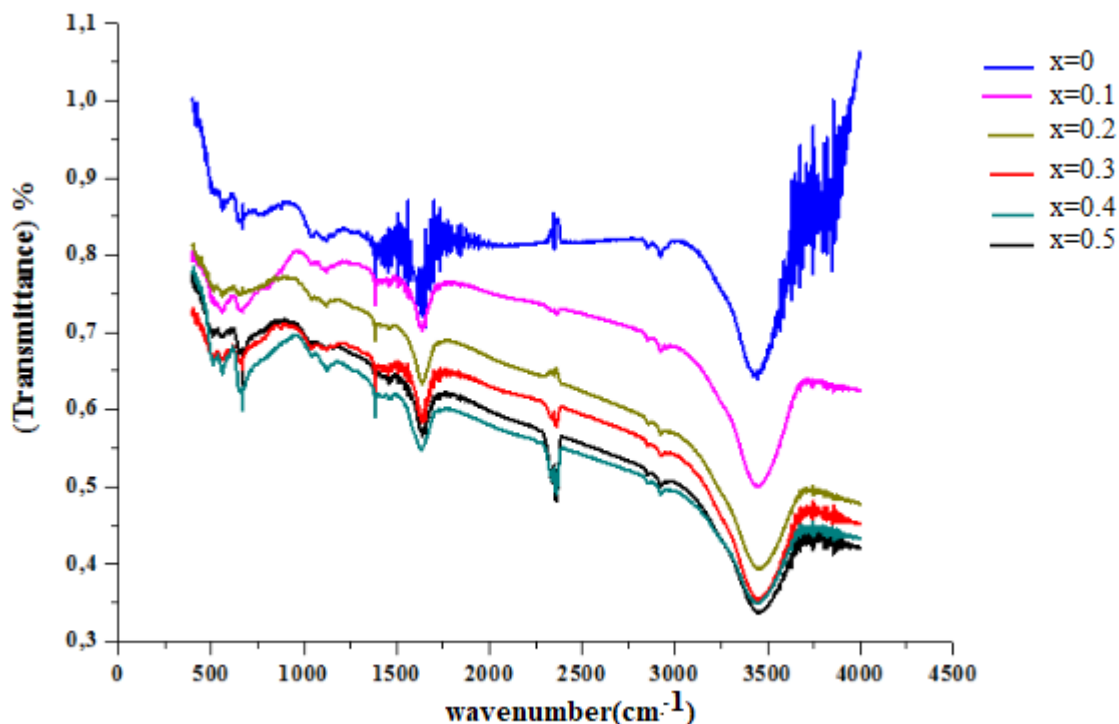
Figure 5: FTIR spectra of $Zn_{1-x}Pb_xBi_2O_4$ compounds (x = 0, 0.1, 0.2, 0.3, 0.4, 0.5)

The results of Infrared light Transmittance of various $Zn_{1-x}Pb_xBi_2O_4$ spinels summarized in Table 4 show clearly that the transmittance decreases with the increase in concentration of Pb in the spinel, since the lead serves as protection against radiation to attenuate X-rays and gamma rays which have a high energy due to its density and its absorbing properties, so it can easily attenuate the infrared light radiation that has low energy. This result is in agreement with the cell volume on crystalline structure of each compound, because the cell volume decrease for some sample with the increase of concentration of Pb in the $Zn_{1-x}Pb_xBi_2O_4$ (x = 0.1and 0.3), after this decreases the materials become denser and more absorbent of light which explains the decrease of the transmittance.

Table 4: Infrared light Transmittance of various $Zn_{1-x}Pb_xBi_2O_4$ spinels.

Wavenumber (cm^{-1})	$Zn_{1-x}Pb_xBi_2O_4$ Powders Transmittance (T %)						Error of all T% ±	Spectral form
	x=0.0	x=0.1	x=0.2	x=0.3	x=0.4	x=0.5		
562	0,87	0,74	0,75	0,65	0,65	0,7	0.01	wide
620	0,83	0,74	0,75	0,64	0,63	0,63	0.01	wide
1375	0,78	0,75	0,68	0,62	0,45	0,65	0.01	delicate
1625	0,75	0,7	0,64	0,55	0,58	0,54	0.01	wide
2340	0,81	0,73	0,65	0,58	0,54	0,45	0.01	delicate
2280	0,78	0,77	0,63	0,54	0,48	0,44	0.01	delicate
3440	0,65	0,55	0,38	0,35	0,34	0,32	0.01	wide

Conclusion

The results obtained from the characterization of XRD made it possible to observe the presence of the single phases of the spinel oxide $Zn_{1-x}Pb_xBi_2O_4$. The substitution of Zn^{2+} by Pb^{2+} exhibit an increase in cell parameters of all powders $Zn_{1-x}Pb_xBi_2O_4$ (x = 0, 0.1, 0.2, 0.3, 0.4, 0.5) and a decrease in transmittance of infrared light. The most striking aspect of the set of samples is their high crystallinity, preferential orientation of the crystallographic planes powders $Zn_{1-x}Pb_xBi_2O_4$, influenced by the preparation technique itself and the operating conditions (chemicals, annealing temperature, etc.). It should also be noted that the widening of the feet of diffraction lines for all powders should be small. Moreover, the presence of shoulders to the left of the lines for the compound $Zn_{1-x}Pb_xBi_2O_4$ is very visible on the diffractogram DRX, which could testify some heterogeneities of crystal phase compositions.

References

1. P. Hajra, S. Shyamal, H. Mandal, P. Fageria, S. Pande, C. Bhattacharya, *Electrochim. Acta*. 123 (2014) 494–500.
2. B. Naik, S. Martha, K.M. Parida, *Int. J. Hydrog. Energy*. 36 (2011) 2794–2802.
3. S.M.F. Shaikh, G. Rahman, R.S. Manea, O.S. Joo, *Electrochim. Acta*. 111 (2013) 593–600.
4. M. Raileanu, M. Crisan, I. Nitoi, A. Ianculescu, P. Oancea, D. Crisan, L. Todan, *Water. Air. Soil. Pollut*. 224 (2013) 1548.
5. A.M. Abdulkarem, J. Li, A.A. Aref, L. Ren, E.M. Elssfah, H. Wang, Y. Ge, Y. Yu, *Mater. Res. Bull*. 46 (2011) 1443–1450.
6. W. Zhang, J. Zhang, Z. Chen, T. Wang, *Catal. Commun*. 10 (2009) 1781–1785.
7. X. Wang, J. Hu, W.Liu, G.Wang, J. An, J. Lian, *J. Mater. Chem*. A. 3 (2015) 23333-23344.
8. S. Chen, Y. Hu, L. Ji, X. Jiang, X. Fu, *Appl. Surf. Sci*. 292 (2014) 357–366.
9. L. Cheng, Y. Kang, *J. Alloys. Compd*. 585 (2014) 85–93.
10. T.G. Glover, J.B. DeCoste, D. Sabo, Z.J. Zhang, *Langmuir*. 29 (2013) 5500–5507.
11. P. Malathy, K. Vignesh, M. Rajarajan, A. Suganthi, *Ceram. Int*. 40 (2014) 101–107.
12. A.K. Chakraborty, S.B. Rawal, S.Y. Han, S.Y. Chai, W.I. Lee, *Appl. Catal. A*. 407 (2011) 217-223.
13. N. Khakpash, A. Simchi, T. Jafari, *J. Mater. Sci. Mater. Electron*. 23 (2012) 659-667.
14. G. Zhang, B.Y. Xia, C. Xiao, L.Yu, X. Wang, Y. Xie, X.W. Lou, *Angew. Chem. Int. Ed*.125 (2013) 8805 - 8809.
15. S.Y. Chai, Y.J. Kim, M.H. Jung, A.K. Chakraborty, D. Jung, W.I. Lee, *J. Catal*. 262 (2009) 144-149.
16. J. Zhang, Y. Jiang, W. Gao, H. Hao, *J. Mater. Sci. Mater. Electron. 26* (2015), 1866-1873.
17. Y. Yang, S. Jayaraman, G.S. Girolami, J.R. Abelson . *J. Cryst. Growth*, *294*(2006) 389-395.
18. R. Kern. *Cryst. Res. Technol*, *48*(2013), 727-782.
19. A. Käppler, F. Dieter, O. Sonja, S. Gerald, L.Matthias, E.K. Jochen, V. Brigitte, *Anal. Bioanal. Chem* 408, 29 (2016) 8377-8391.
20. G. Dayal, X.Y. Chin, C. Soci, R. Singh, *Adv. Opt. Mater* 5, 2 (2017) 1600559.
21. A. Dazzi, C.B. Prater, *Chem. Rev* 117, 7 (2016) 5146-5173.

(2018) ; http://www.jmaterenvironsci.com